

Electronic Supplementary Information:

1,3-diiodobenzene on Cu(111) –  
an exceptional case of on-surface Ullmann coupling

Atena Rastgoo Lahrood<sup>a,b</sup>, Jonas Björk<sup>c</sup>, Wolfgang M. Heckl<sup>a,b,d</sup>, and Markus Lackinger<sup>a,b,d\*</sup>

<sup>a</sup> Department of Physics, Technische Universität München, James-Franck-Str. 1, 85748 Garching, Germany.

<sup>b</sup> Nanosystems-Initiative-Munich and Center for Nanoscience, Schellingstrasse 4, 80799 München, Germany.

<sup>c</sup> Department of Physics Chemistry and Biology, IFM Linköping University 58183 Linköping, Sweden.

<sup>d</sup> Deutsches Museum, Museumsinsel 1, 80538 München, Germany.

\*Tel: +49 89 2179-605; email: markus@lackinger.org

## 1. Experimental details

All scanning tunneling microscopy (STM) data were acquired with a home-built beetle type STM driven by a SPM100 controller from RHK. Images were recorded at room temperature in ultra-high vacuum at a base pressure below  $3 \times 10^{-10}$  mbar. The bias voltage is applied from the sample to the tip. The STM was calibrated by means of atomically resolved Cu(111) images. This facilitates extraction of lattice parameters and distances with an accuracy of  $\sim 5\%$ . STM images were processed by a mean value filter. Cu(111) single crystal surfaces were prepared by cycles of Ne<sup>+</sup> ion-sputtering at 1 keV and electron-beam annealing at  $\sim 773$  K. The surface cleanliness was verified by STM imaging before deposition. 1,3-diiodobenzene (DIB, CAS 626-00-6, obtained from Sigma Aldrich, purity 98%) was dosed through a precision leak valve, equipped with a stainless steel capillary aiming at the sample.

## 2. Computational Details

Periodic density functional theory (DFT) calculations were performed with the VASP code,[Kresse1996] using the projector-augmented wave method [Blöchl1994] to describe ion-core interactions. Exchange-correlation were described by the van der Waals density functional (vdW-DF),[Dion2004, Thonhauser2007] in the recent form by Hamada,[Hamada2014] denoted by rev-vdW-DF2, which has shown to accurately describe molecular adsorption in a variety of systems.[Hamada2014, Björk2014]

### Trimers on I/Cu(111)

The Cu(111) surface was represented by a slab geometry of four layers. The iodine overlayer was placed in the known superstructure [Citrin1980]. A  $p(5 \times 6)$  surface unit cell was used (with respect to the primitive unit cell of the iodine overlayer). Furthermore, we used a  $2 \times 2$  k-point sampling, and a 400 eV kinetic energy cutoff. STM simulations were performed with the Tersoff-Hamann approximation,[Tersoff-Hamann1983] using the implementation by Lorente and Persson.[Lorente-Persson2000]

### Benzene-1,3-diradical on Cu(111) and Cu(110)

For the calculations of the benzene-1,3-diradical, a  $p(6 \times 6)$  unit cell was used for Cu(111) and a  $p(4 \times 6)$  unit cell for Cu(110) (6 atoms in the close-packed direction). In both cases a  $4 \times 4$  k-point sampling was used, which ensured convergence of adsorption energies within 50 meV. Both surfaces were represented by four layers slabs, where the outermost two layers were allowed to fully relax.

### References:

[Kresse1996] G. Kresse and J. Furthmüller, Phys. Rev. B 1996, 54, 11169

[Blöchl1994] P. E. Blöchl, Phys. Rev. B 1994, 50, 17953

[Dion2004] M. Dion, H. Rydberg, E. Schröder, D. C. Langreth and B. I. Lundqvist, Phys. Rev. Lett. 2004, 92,

[Thonhauser2007] T. Thonhauser, V. R. Cooper, S. Li, A. Puzder, P. Hyldgaard and D. C. Langreth, Phys. Rev. B 2007, 76, 125112

[Hamada2014] I. Hamada, Phys. Rev. B 2014, 89, 121103(R)

[Björk2014] J. Björk and S. Stafström, ChemPhysChem 2014, 15, 2851

[Citrin1980] P. H. Citrin, P. Eisenberger and R. C. Hewitt, Phys. Rev. Lett. 1980, 45, 1948

[Tersoff-Hamann1983] J. Tersoff and D. Hamann, Phys. Rev. Lett. 1983, 50, 1998

[Lorente-Persson2000] N. Lorente and M. Persson, Faraday Discuss. 2000, 117, 277

### 3. Additional DFT results and STM image simulations

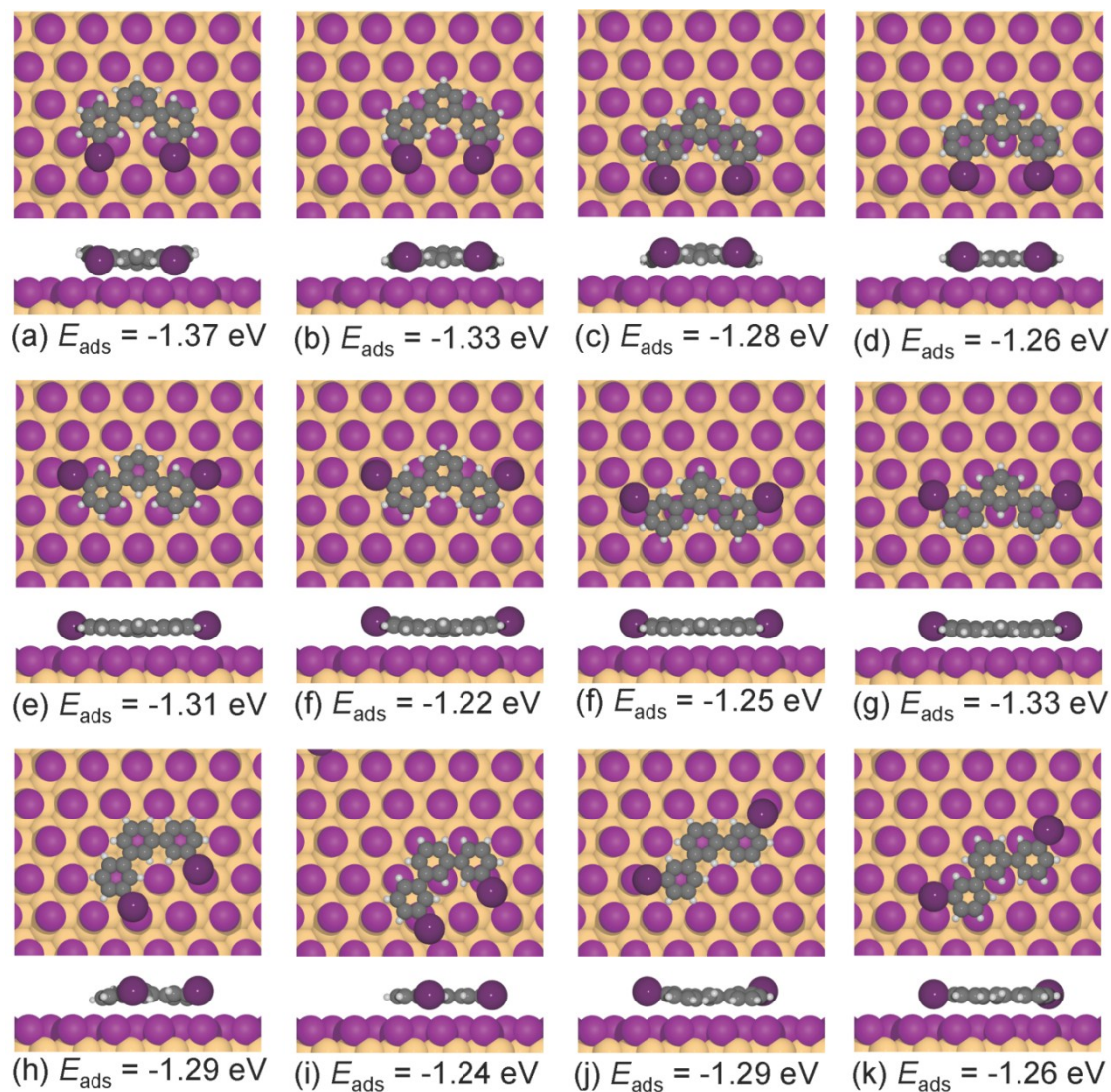


**Fig. S1** (a) – (k): Top and side views of DFT optimized adsorption geometries of iodinated trimers on top of a close packed iodine  $\sqrt{3}\times\sqrt{3}$  R30° superstructure on Cu(111). The adsorption energies, calculated with respect to isolated and surface-adsorbed molecule, are indicated below the respective structures. Structure (a) results in the lowest adsorption energy. However, energy differences between the different adsorption geometries studied here are relatively small, indicating a low surface diffusion barrier.

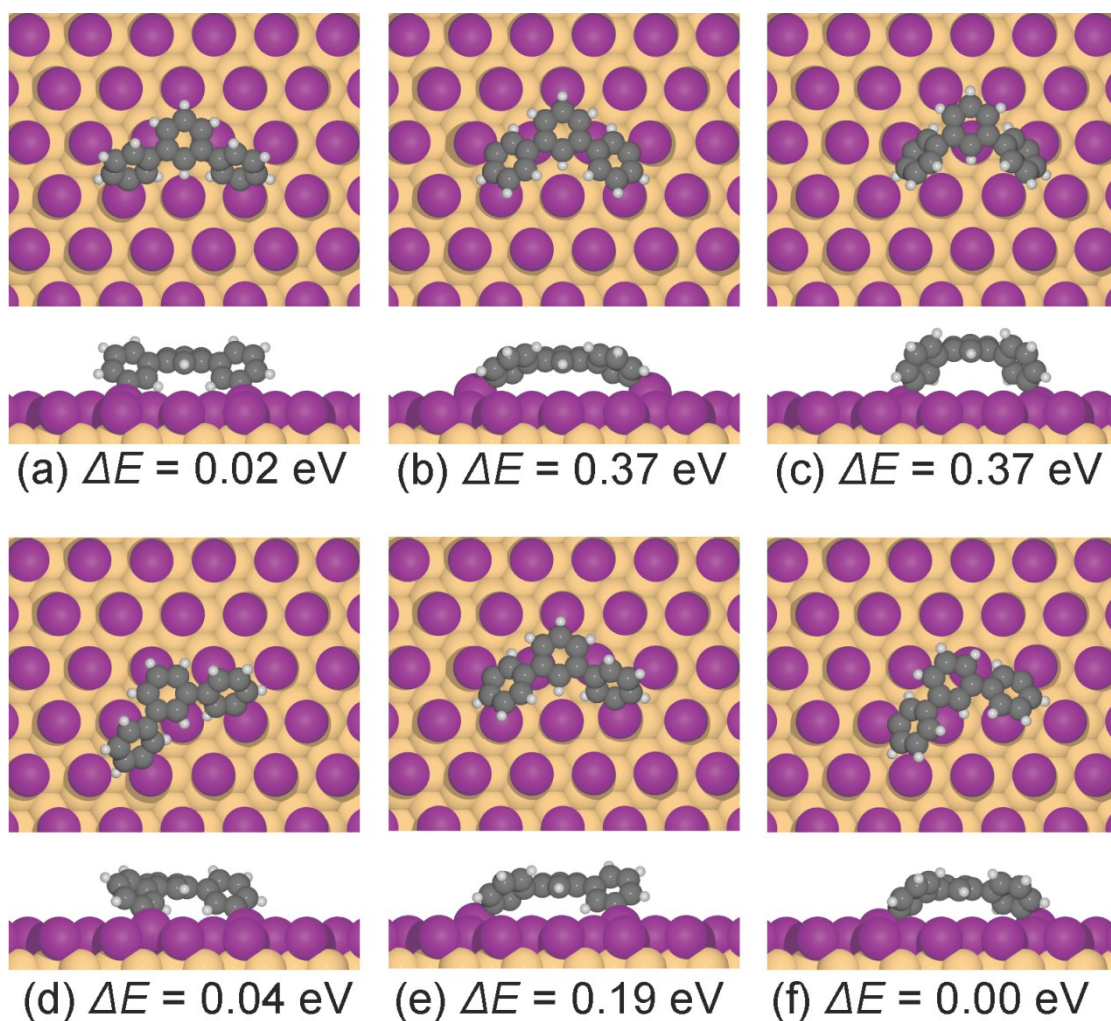


**Fig. S2** (a) – (f): Top and side views of DFT optimized adsorption geometries of deiodinated (diradicalic) trimers on top of a close packed  $\sqrt{3}\times\sqrt{3}$  R30° iodine superstructure on Cu(111). Structure (f) results in the lowest energy. The energy differences  $\Delta E$  with respect to the most stable geometry (f) are indicated below each structure.

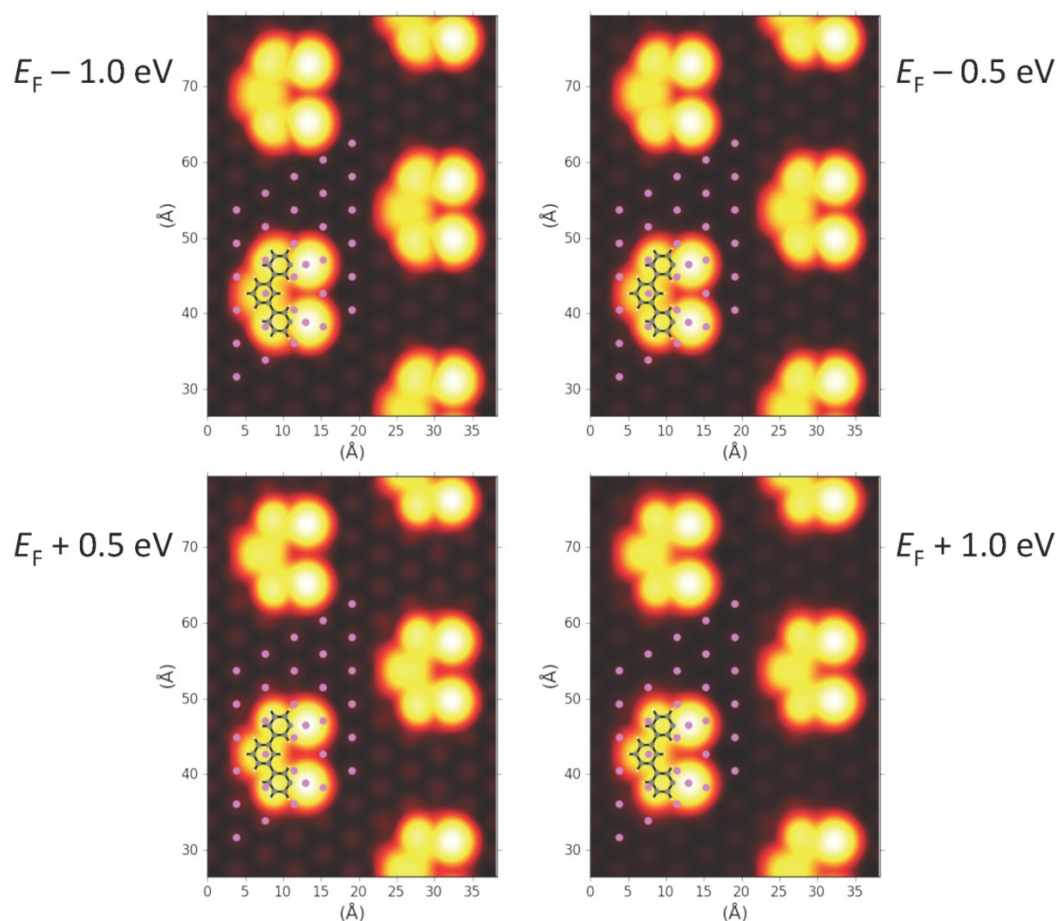


**Fig. S3** STM image simulations of iodinated trimers based on the lowest energy structure (cf. Fig. S1(a)). Electronic sample states were considered between the Fermi energy ( $E_F$ ) and the respective energies stated on the margin; Accordingly, the upper row depicts STM image simulations of occupied electronic states (negative sample bias), whereas the lower row depicts STM image simulations of unoccupied electronic states (positive sample bias). The STM contrast was found to be virtually independent of sample bias and polarity.



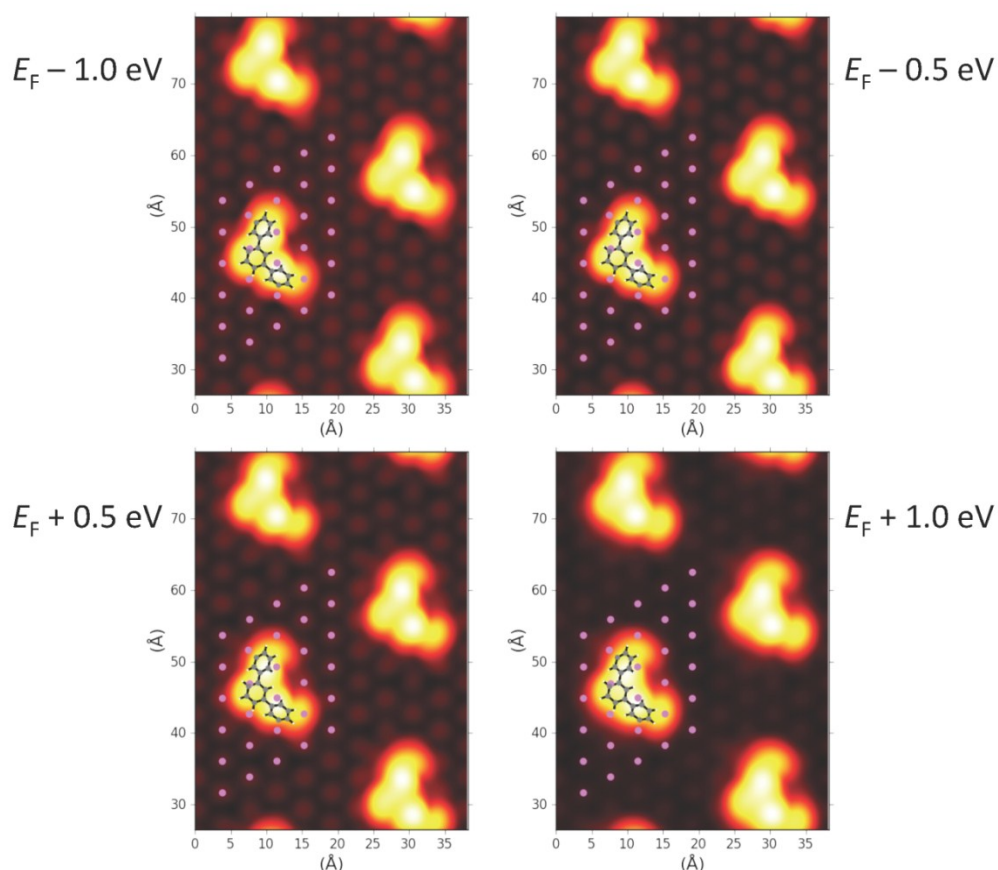


**Fig. S4** STM image simulations of deiodinated (diradicalic) trimers based on the lowest energy structure (cf. Fig. S2(f)). Electronic sample states were considered between the Fermi energy ( $E_F$ ) and the respective energies stated on the margin; Accordingly, the upper row depicts STM image simulations of occupied electronic states (negative sample bias), whereas the lower row depicts STM image simulations of unoccupied electronic states (positive sample bias). The STM contrast was found to be virtually independent of sample bias and polarity.

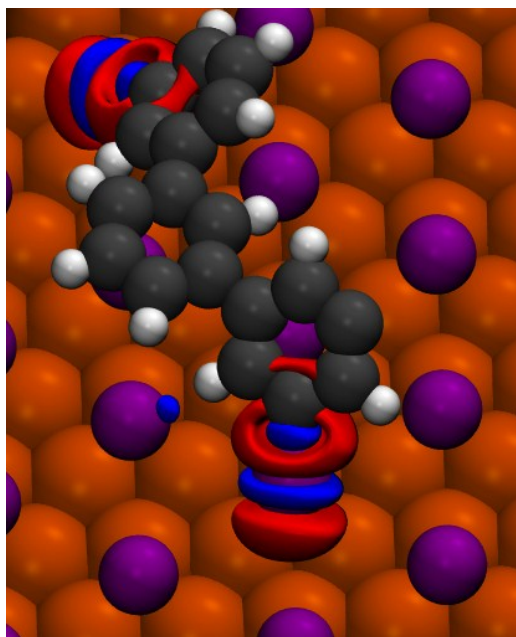


**Fig. S5** Electron density difference plot, showing the electron redistribution due to adsorption of the diradicalic trimer on the close packed  $\sqrt{3}\times\sqrt{3}$  R30° iodine superstructure on Cu(111). The blue and red contours show electron accumulation and depletion, respectively. The absolute value of the contours is  $0.01 \text{ e}/\text{\AA}^3$ .

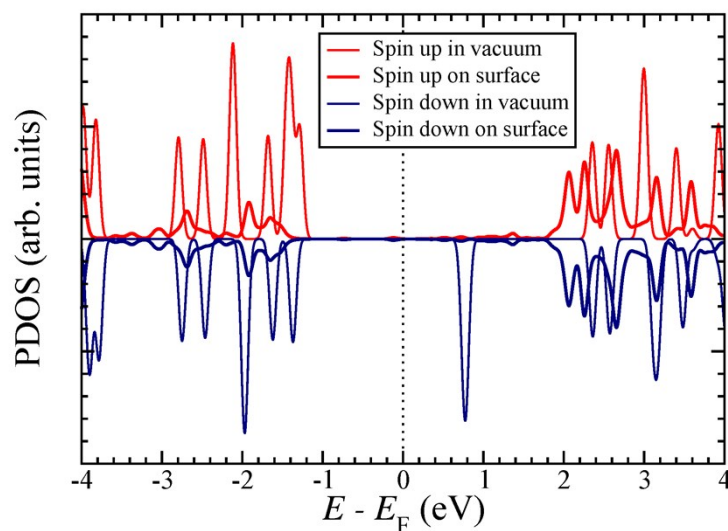


**Fig. S6** Partial density of states (PDOS) on the carbon atoms of the diradicalic trimer in vacuum and adsorbed on the close packed  $\sqrt{3}\times\sqrt{3}$  R30° iodine superstructure on Cu(111). The vacuum levels of both systems were aligned, and the Fermi energy ( $E_F$ ) refers to the surface. By coincidence, occupied and unoccupied states of the isolated molecule are below and above this Fermi energy, respectively. In vacuum, the spins of the diradicalic trimer are unpaired, but become paired upon adsorption due to interactions with the surface. The frontier orbitals are strongly hybridized, indicating the covalent character of the bond between the radical sites and the surface-bound iodine atoms.

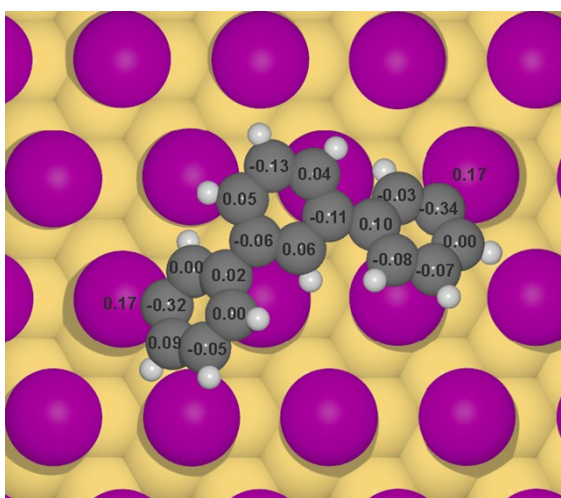


**Fig. S7** Atom-wise Bader charge analysis of the carbon atoms of the deiodinated (diradicalic) trimer and the two adsorbed iodine atoms bonded to the trimer. The lowest energy structure was used (cf. Fig. S2(f)) and charges are given in units of  $e$ . The total charge of the molecule (including H atoms, but excluding the adsorbed iodine atoms) is  $-0.24 e$ . Notable, the two iodine atoms bonded to the trimer have positive Bader charges of  $+0.17 e$  each. In contrast, all other adsorbed iodine atoms have negative Bader charges in the range  $-0.23 e$  to  $-0.26 e$ . The local positively charged character of the iodine atoms bonded to the trimer might partly explain the repulsion between trimers.

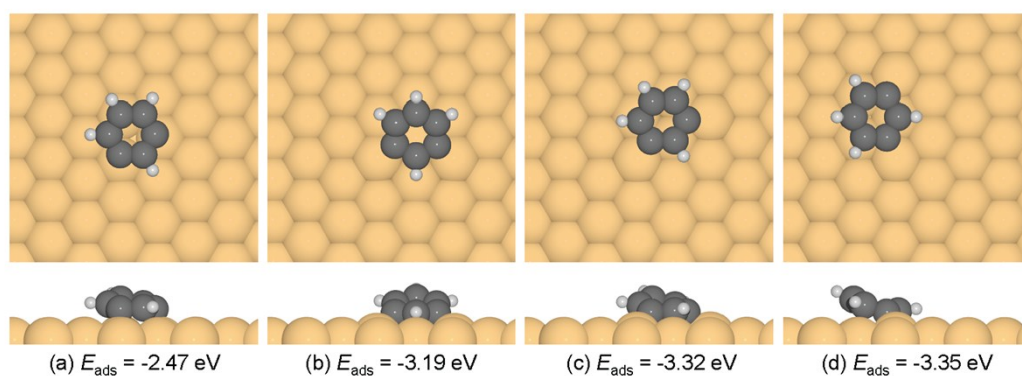


**Fig. S8** Top and side views of DFT optimized adsorption geometries of the benzene-1,3-diradical on Cu(111). The adsorption energies, calculated with respect to isolated and surface-adsorbed molecule, are indicated below the respective structures. The most stable adsorption geometry is shown in (d).

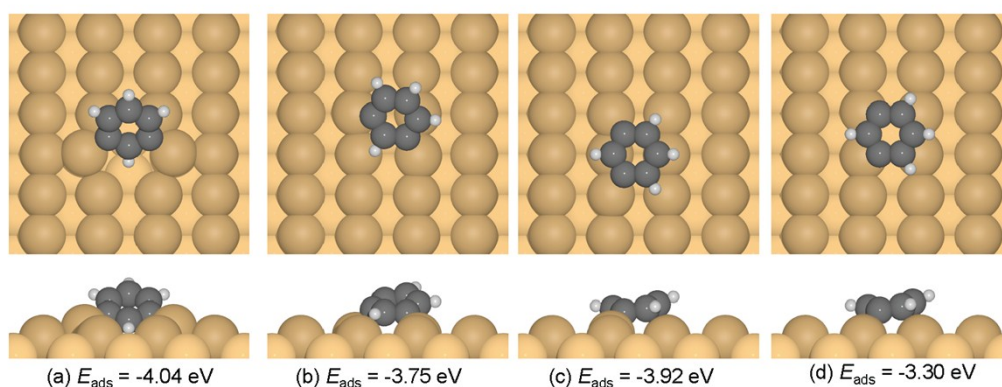


**Fig. S9** Top and side views of DFT optimized adsorption geometries of the benzene-1,3-diradical on Cu(110). The adsorption energies, calculated with respect to isolated and surface-adsorbed molecule, are indicated below the respective structures. The most stable adsorption geometry is shown in (a).



## 4. Additional STM results

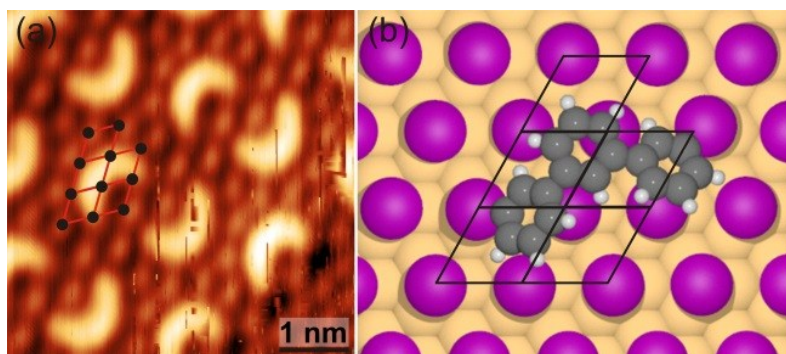


**Fig. S10** (a) STM image ( $V=+0.84$  V,  $I=39$  pA) and (b) DFT derived lowest energy structure (cf. Fig. S2(f)) of the deiodinated trimer. Experiment and simulation consistently result in the same orientation of the trimer with respect to the hexagonal iodine superstructure.

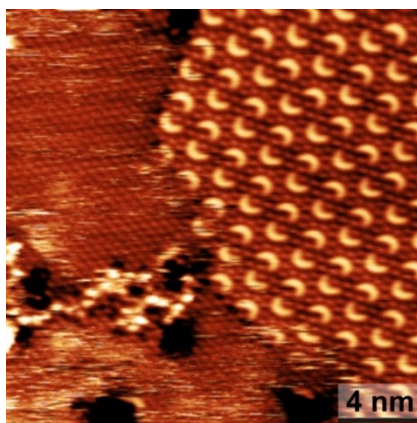


**Fig. S11** STM image ( $V=+0.84$  V,  $I=39$  pA) showing a domain boundary of the self-assembled trimer structure. Adjacent to the self-assembled domain, the surface is solely covered by the close packed iodine superstructure. Since the amount of iodine is already overstoichiometric in the self-assembled structure, this observation indicates an even larger excess of iodine on the surface.

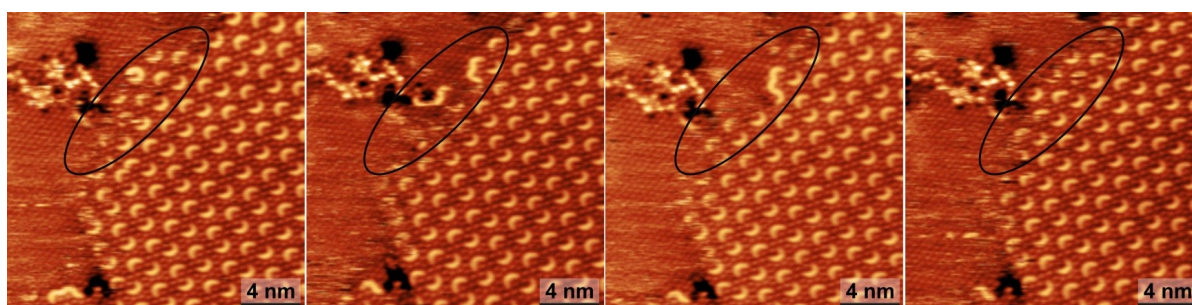


**Fig. S12** Series of STM images consecutively acquired from the same sample area (from left to right;  $V=+0.84$  V,  $I=39$  pA). The black oval highlights dynamic processes observed at domain edges, including lateral mobility of trimers and coupling of trimers into larger, less well defined aggregates.



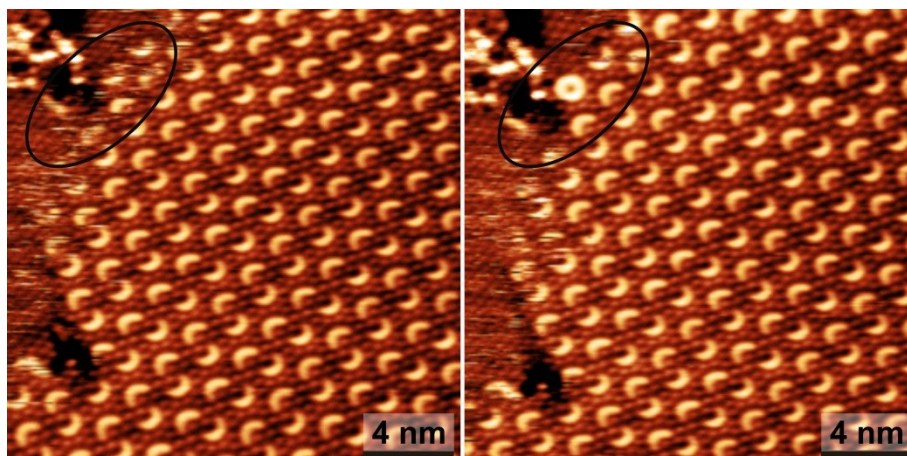


**Fig. S13** Two STM images consecutively acquired from the same sample area ( $V=+0.84$  V,  $I=39$  pA). The black oval highlights the appearance of a closed ring, i.e. cyclo-sexiphenylene, in the second image. A conclusion whether this ring has formed on-site by coupling of two trimers or whether it diffused to this site is not possible based on these STM experiments.

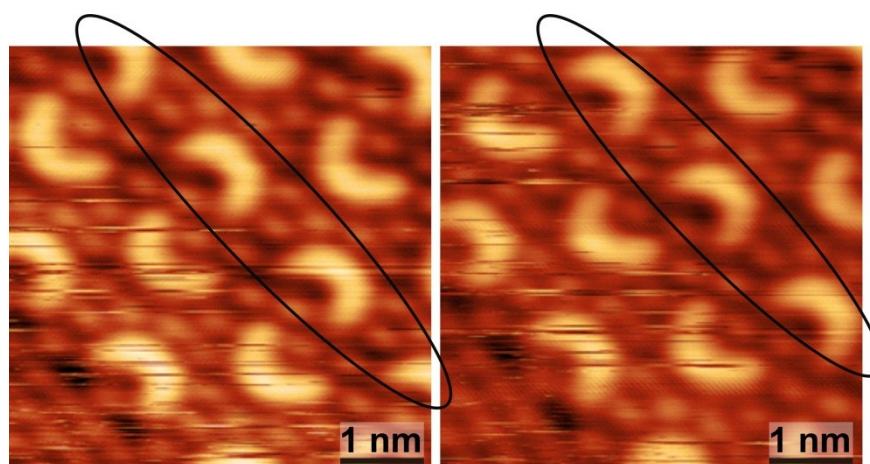


**Fig. S14** Two STM images consecutively acquired from the same sample area ( $V=+0.84$  V,  $I=39$  pA). The black oval highlights lateral displacement of a row of trimers as a whole. This concerted movement of trimer rows indicates an effective long-range interaction as also required for self-assembly of the observed patterns.

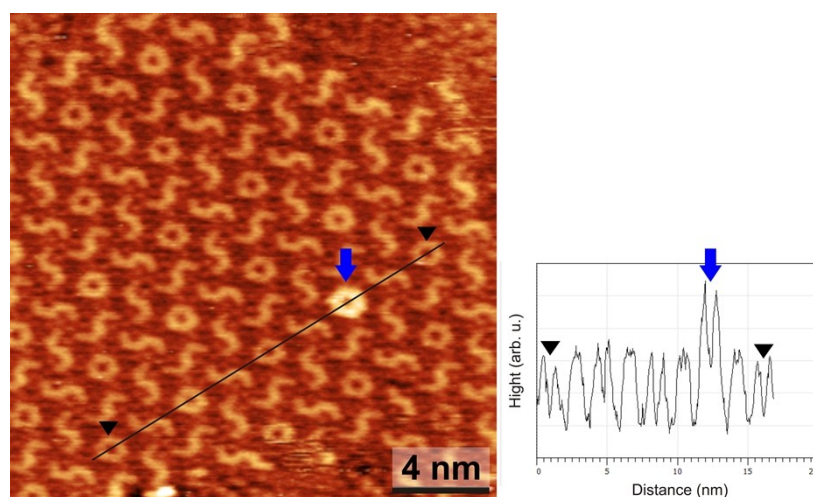


**Fig. S15** Overview STM image of the occasionally observed more complex structure. ( $V=+0.81$  V,  $I=38$  pA). This self-assembled structure is comprised of two different hexamers: closed rings that are surrounded by a hexagonal arrangement of S-shaped entities. Interestingly, the closed ring marked by the arrow appears significantly brighter, i.e. higher than all others. Since both geometry and adsorption site are similar to all other rings, we speculate that two rings are stacked on top of each other. The line profile on the right side indicates that the brighter ring marked by the blue arrow has about twice the height of all other rings.